Talanta 83 (2010) 55–60

Contents lists available at ScienceDirect

Talanta

journal homepage: www.elsevier.com/locate/talanta

A newly developed immunoassay method based on optical measurement for Protein A detection

Chia-Hsien Yeh[a], Wei-Ting Chen[a], Hong-Ping Lin[b], Tsung-Chain Chang[c], Yu-Cheng Lin[a,*]

[a] Dept. of Engineering Science, National Cheng Kung University, 1 University Road, Tainan 701, Taiwan
[b] Dept. of Chemistry, National Cheng Kung University, Tainan, Taiwan
[c] Dept. of Medical Laboratory Science and Biotechnology, National Cheng Kung University, Tainan, Taiwan

ARTICLE INFO

Article history:
Received 22 June 2010
Received in revised form 20 August 2010
Accepted 24 August 2010
Available online 19 September 2010

Keywords:
Immunoassay
Silver enhancement reaction
Flatbed scanner
Grayscale

ABSTRACT

We describe the development of an immunoassay using an antibody–silver nanoparticle (Ab–AgNP) conjugate as a catalyst for the silver enhancement reaction. The immuno-reaction signals that were magnified by silver metal precipitation were quantified using a commercial flatbed scanner. Protein A from *Staphylococcus aureus* (*S. aureus*), a common clinical pathogenic bacterium, was used in this research. The ease of infection of *S. aureus* necessitates the development of a fast detection method. The framework of the method described in this paper is based on the sandwich immunoassay and contains a 1st antibody (immunoglobulin G, IgG), an antigen (Protein A), and a 2nd antibody–colloidal silver conjugate (IgG–AgNPs). The silver enhancement reaction, a signal amplification method in which silver ions are reduced to metallic silver, is used to magnify the immuno-reaction signal. The change in signal, as visualized in grayscale, can be easily observed and analyzed by our optical scanning detection system. The relationship between antigen concentration and grayscale value is discussed. The detectable concentration limit for the antigen was found to be 1 ng/mL with 10 μg/mL of IgG and 300 μM of the IgG–AgNP conjugate. This immunoassay method provides the advantages of low cost, easy operation, and short detection time. Moreover, it has potential applications in clinical diagnoses.

1. Introduction

The immunoassay is based on a specific interaction between an antibody and a complementary antigen and is a powerful analytical method for clinical diagnoses and environmental monitoring. Based on the material used for protein labeling, an immunoassay can be classified as an enzyme immunoassay (EIA) [1,2], a fluorescent immunoassay (FIA) [3,4], or a chemiluminescence immunoassay (CLIA) [5,6]. The most commonly used format of immunoassay is the enzyme-linked immunosorbent assay (ELISA), a technique for detecting an antibody or antigen in a sample. In the ELISA, an enzyme that is linked to an antibody or antigen is used as a marker. The antibody-conjugated enzyme reacts with a colorless substrate to produce colored products that can be measured by an ELISA reader [7,8]. In the conventional immunoassay, expensive instruments (e.g., ELISA readers) and complex processes limit the application of this method.

In recent years, metallic colloid nanoparticles have been used in labeling technology because of their easily controllable size, uniqueness, and high biocompatibility with antibodies, proteins, RNA, and DNA [9–16]. Due to the surface plasma absorption of nanoparticles, proteins labeled with colloid gold were observed by transmission electron microscopy (TEM) [17,18] and were analyzed by surface enhanced Raman spectroscopy (SERS) [19,20]. In immunogold silver staining (IGSS), the reduction response reduces the silver ions in the silver enhancement solution to metallic silver, a reaction that is catalyzed by gold nanoparticles (AuNPs). The precipitation of silver metals occurs on the surface of the nanoparticles, and experiments have been performed to optimize the detection signals [11,21]. For example, Mirkin et al. used a simple commercial flatbed scanner to detect the colorimetric change associated with DNA hybridization in his experiment in which a nanogold probe was coupled with the silver enhancement method [16]. In addition, Alexandre et al. implemented DNA microarray detection with a colorimetric-based workstation containing a charge-coupled device (CCD) camera [22].

AuNPs have been used as targets in immunoassays [16,22–24], but silver nanoparticles (AgNPs) are also excellent prospects for biological sensing [25]. AgNPs are desirable as targets in electrochemical detection assays because they have better electrochemical activity than AuNPs, the electrochemical redox reaction of AgNPs is carried out at a low potential (under 0.4 V), and they give a well-defined sharp voltammetric peak. The oxidative peak of colloid silver is approximately 100 times larger than that for colloid

* Corresponding author. Tel.: +886 6 276 2395; fax: +886 6 276 2329.
E-mail address: yuclin@mail.ncku.edu.tw (Y.-C. Lin).

0039-9140/$ – see front matter © 2010 Elsevier B.V. All rights reserved.
doi:10.1016/j.talanta.2010.08.038

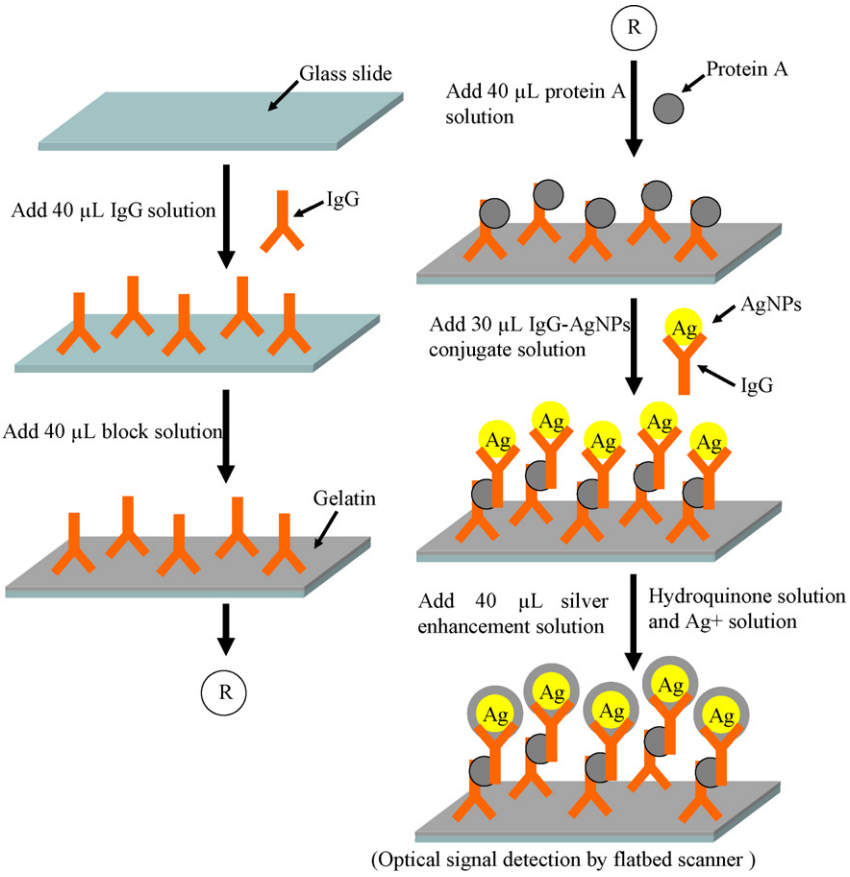

Fig. 1. Schematic representation of our newly developed sandwich immunoassay (three-layer format) in which silver ions are reduced to metallic silver on the AgNP surface by AgNP catalysis.

gold of the same size and mass [26,27]. Moreover, the absorption factor of the AgNP surface is 4-fold that of the AuNP surface [28]. Therefore, AgNPs could be better catalysts and, thus, replace the role of AuNPs in immunoassays [29].

The general method of antibody–antigen conjugation is to conjugate the antigen to the Fab or Fc region of the antibody. Binding of the antigen to the Fab or Fc region of immunoglobulin G (IgG) is a commonly used method, as well. Both Fab and Fc conjugation methods involve the binding of the antibody to the antigen; the difference only lies in the binding interaction itself. The bond with the Fab region is a hydrophobic interaction, whereas that with the Fc region is a covalent bond, both of which are stable interactions. In this study, the antigen (Protein A) was bound to the Fc region of the antibody (IgG), which is a commonly used method [30,31]. *Staphylococcus aureus* (*S. aureus*) is a pathogenic bacterium that causes human infection and intoxication. The detection of this bacterium is very important in clinical diagnoses. Protein A produced by *S. aureus* can bind the Fc region of IgG without interfering with the binding sites of the antigen, making it very attractive for immunoassay applications.

In this study, an AgNP label and the silver enhancement reaction were used in a sandwich immunoassay (three-layer format), as shown in Fig. 1. Protein A (from *S. aureus*) and IgG (from human) were selected as models due to their high specificity and convenience [32]. IgG–AgNP conjugates were used as targets to catalyze the reduction of silver ions in the enhancement solution to metallic silver, resulting in an increase in particle size and in color differentiation. The change in the grayscale value produced from the immuno-reaction with various antigen concentrations was observed both by the naked eye and with an optical scanning detection system. After the proper conditions were established on a glass slide, a flatbed scanner was used to capture the optical signals (grayscale), which were then processed on a personal computer for data analysis using Adobe Photoshop® software. The concentration effect and detectable concentration limit were determined for this sandwich immunoassay experiment.

2. Materials and methods

2.1. Reagents

Silver nitrate ($AgNO_3$), human serum IgG, anti-human IgG (Protein A), phosphate-buffered saline (PBS), and silver enhancement solution A (silver salt) and B (hydroquinone initiator) from the Silver Enhancer Kit were purchased from Sigma–Aldrich (St. Louis, MO, USA). Sodium citrate (dehydrate, granular) was obtained from J.T. Baker (Mexico). Sodium borohydride powder (98%) was obtained from ACROS (Belgium, China). Bovine serum albumin (BSA) was purchased from Roche (Mannheim, Germany).

2.2. Principle of the sandwich immunoassay

Our newly developed method utilizes a sandwich immunoassay and signal amplification method and is designed for qualitative and quantitative analyses. A schematic representation is shown in Fig. 1. For our sandwich immunoassay, the 1st antibody (IgG) was immobilized on a glass slide and then the antigen (Protein A) was bound to the 1st antibody. Next, the 2nd antibody–AgNP conjugate (IgG–AgNP conjugate) was bound to the antigen, which was bound to the 1st antibody.

For signal amplification, the reaction in which silver ions in the silver enhancement solution were reduced to metallic silver

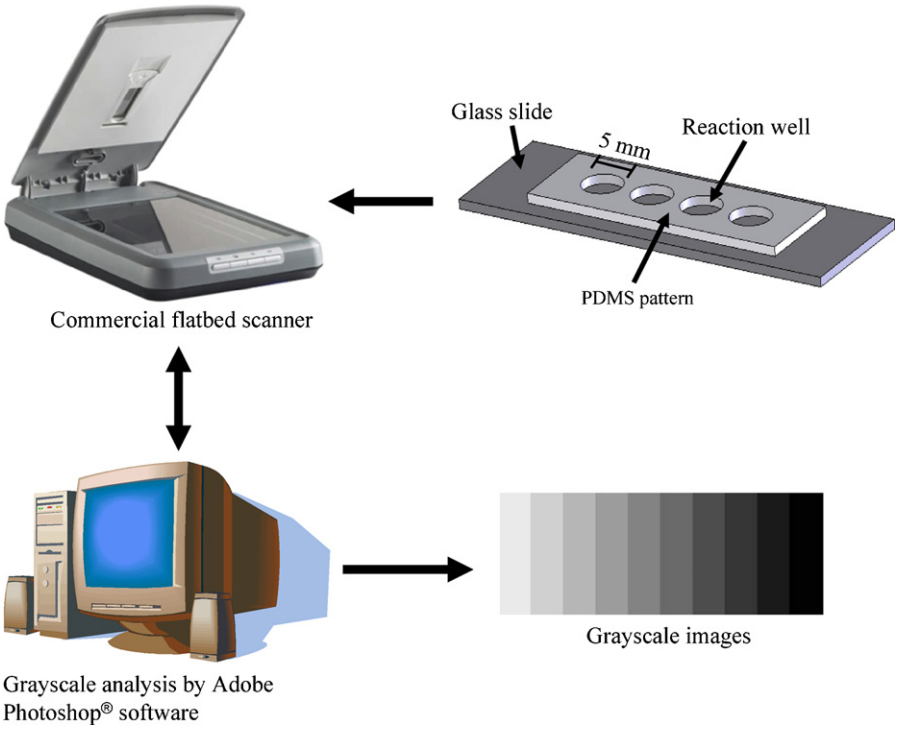

Fig. 2. Silver precipitation immunoassay detection. Circular reaction wells were formed using PDMS. After the immuno-reaction and silver enhancement reaction, the detection signals were measured with a flatbed scanner. Adobe Photoshop® software was used to analyze the grayscale values of the detection signals.

was catalyzed by AgNPs. A large amount of silver precipitate was observed around the surface of the AgNPs. The silver precipitation generated optical signals that were detected by a commercial flatbed scanner, and the relationship between the grayscale change and antigen concentration was determined. In the silver enhancement reaction, the silver enhancement solution used was a mix of the "Ag+ solution" and the "hydroquinone solution" at a 1:1 ratio. The chemical reactions are as follows:

$$\text{Hydroquinone} \xrightarrow{\text{AgNPs}} \text{Benzoquinone} + 2e^- + 2H^+ \quad (1)$$

$$Ag^+ + e^+ \rightarrow Ag \quad (2)$$

According the equations, silver nanoparticles catalyze silver ions reduction by hydroquinone. The hydroquinone has quickly released the electrons by the AgNPs catalysis. The silver ions in the silver enhancement solution are reduced to silver metals by accepting the electrons, and a large number of silver particles are precipitated around the AgNPs.

2.3. Synthesis of silver nanoparticles

Silver nanoparticles (10 nm) were prepared using a modified citrate reduction process [36,37]. In a typical experiment, 10 mL of 170 mM sodium citrate was added to 100 mL of 1.016 mM $AgNO_3$. Then, 20 mL of 10.576 mM $NaBH_4$ was dropped into the sodium citrate/$AgNO_3$ solution with stirring at 0 °C. The resultant yellow solution contained 10 nm AgNPs. No precipitate was observed, even after a few days of storage, as shown in Fig. 3(c). The concentration of the AgNPs using the spherical model was:

$$C = \frac{\text{concentration of } Ag^+ \text{ in the precursor solution}}{\text{the number of Ag atoms in each AgNPs}} = \frac{[Ag^+]}{(4/3)\pi d^3 \times \text{density of Ag/atomic weight of Ag}} \quad (3)$$

C: AgNP concentration; d: radius of AgNPs; density of Ag: 10,500 kg/m^3; atomic weight of Ag: 108 g/mole.

Based on our synthetic composition, the concentration of AgNPs = 0.025 μM. Then, the 10 mL of AgNPs solution was concentrated by centrifugation (Roter AT-2018 M, Kubota Instruments Inc., Japan) at 13,500 rpm (15,465 × g) for 15 min, and then the supernatant was discarded. The concentrated AgNPs solution was adjusted to various concentrations of the AgNPs solution by mixing with the PBS solution.

2.4. Preparation of IgG–AgNP conjugates

When a protein is in a solution with a pH below its isoelectric point (PI), the electric charge of the protein is positive and easily reacts with the negative charge of the AgNP surface. The PI of IgG is close to 8.0, and IgG has good adsorbability to the surface of AgNPs [38]. The pH of the AgNP solution (10 mL) was adjusted to approximately 5.5–6.5 by adding phosphate buffer (PB, 0.01 M, pH 6.5). Then, 1 mL of the IgG solution (10 μg/mL) was slowly mixed with the AgNP solution, and the mixture was stirred until uniform at 4 °C for 3 h. The IgG was adsorbed onto the surface of the AgNPs through ionic interactions. To prevent the IgG–AgNP conjugates from aggregating, 1 mL of a 1% BSA solution was added to the IgG–AgNP solution to separate the nanoparticles and decrease aggregation. The IgG–AgNPs conjugate solution was separated from the mixture by centrifugation at 13,500 rpm (15,465 × g) at 4 °C for 15 min. The IgG–AgNPs conjugate solution was the recovered from the bottom of the mixture. By comparing the absorbance of original AgNPs solution concentration with the absorbance of the IgG–AgNPs conjugate solution, the concentration of the IgG–AgNPs conjugate solution was calculated, and the IgG–AgNPs conjugate solution was adjusted to various concentrations by mixing with the PBS solution. To increase the stability and purity of the IgG–AgNP conjugates, the supernatant (unconjugated solution of AgNPs and IgG) was discarded, and then the resuspended solution mixed with 0.1 mL of 0.1% Triton X-100, 3 mL of 5% sucrose, 3 mL of 1% BSA, and 1 mL of 10 mM PB was added into IgG–AgNPs conjugate solution.

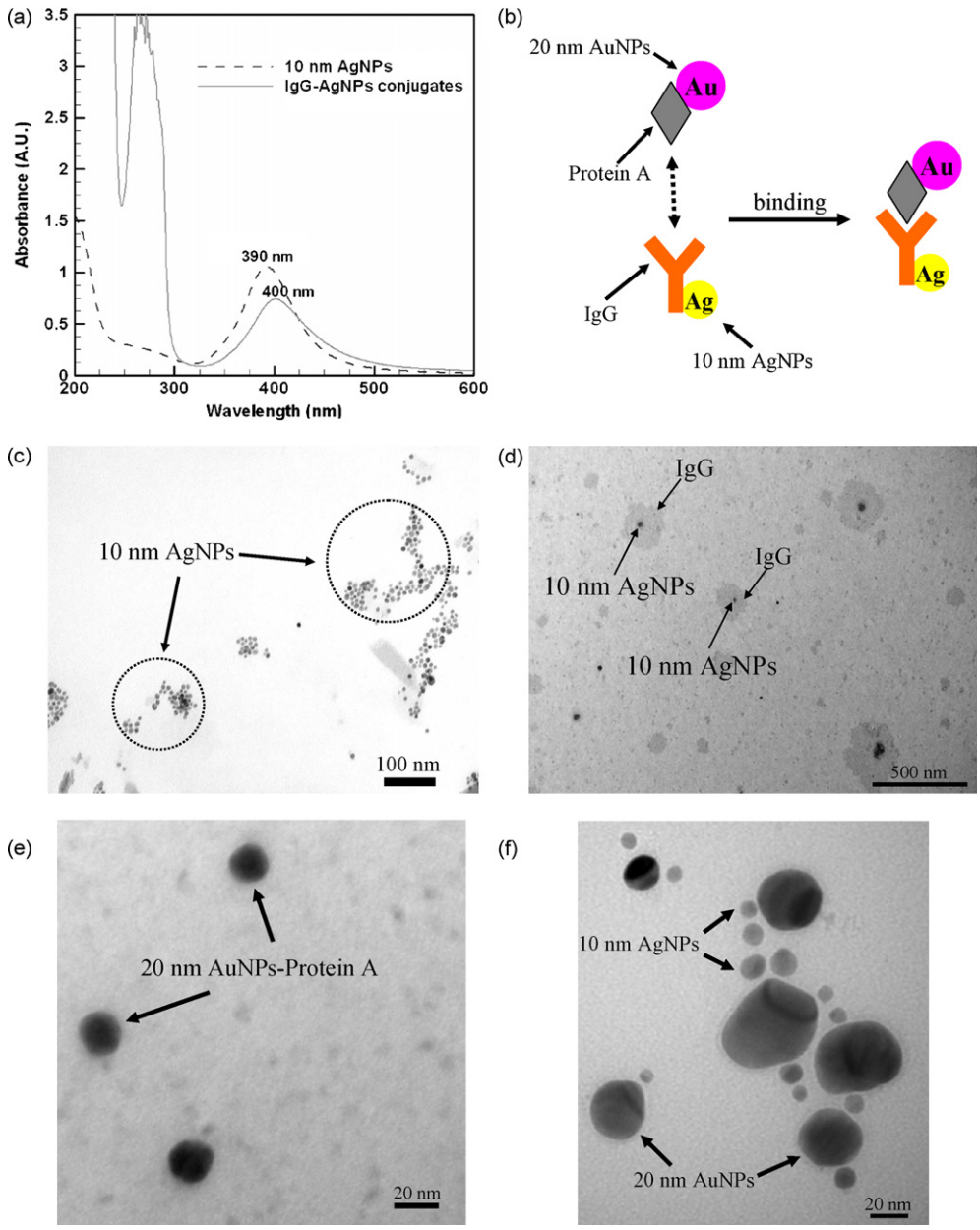

Fig. 3. (a) UV–vis absorption spectrums of 10 nm AgNPs and IgG–AgNP conjugates. (b) Diagram of 20 nm AuNPs conjugated with Protein A and 10 nm AgNPs conjugated with IgG. (c) The TEM photo of 10 nm AgNPs, (d) the TEM photo of 10 nm AgNPs–IgG conjugates, and (e) the TEM photo of 20 nm AuNPs–Protein A conjugates. (f) A specific gap size between the AuNPs and AgNPs was formed when the antibody (IgG) was conjugated to antigen (Protein A), as observed by TEM.

2.5. Experimental procedure

A glass slide was dried with nitrogen gas (N_2) and covered with polydimethylsiloxane (PDMS), which was punched (regular-size hole puncher) to form reaction wells that were 5 mm in diameter. The framework included the sandwich immunoassay procedure and the optical detection procedure, as shown in Fig. 1.

The sandwich immunoassay procedure was performed as follows. First, 40 μL of IgG (10 μg/mL) diluted in PBS (10 mM KH_2PO_4/K_2HPO_4, 150 mM NaCl, pH 7.0) was pipetted onto the glass slide surrounding the PDMS reaction wells. The slide was then incubated for 3 h at 37 °C. After washing twice with PBST (0.01 M PBS and 0.05% Tween 20) and once with deionized water (D.I. water), 40 μL of blocking solution (1% gelatin in PBS) was added to each well and incubated overnight at 37 °C. After washing with PBST and D.I. water, 40 μL of serial 10-fold dilutions of Protein A (diluted in PBS solution containing 1% gelatin) was added to each well and then incubated for 3 h at 37 °C. Finally, after washing with PBST solution and D.I. water, 30 μL of the IgG–AgNP conjugate solution was added to each well and then incubated for 2 h at 37 °C.

The optical detection procedure was performed as follows. Each reaction well on the slide was rinsed with PBST and D.I. water, and 40 μL of the silver enhancement solution was added into the reaction wells. The silver enhancement solution was removed and replaced every 3 min to avoid the natural formation of silver particulate in the silver enhancement solution, but not particulate formed as a result of AgNP catalysis [29]. After washing 3 times with D.I. water and drying with N_2, the optical detection signals were recorded with a flatbed scanner. The relationship between anti-

gen concentration and grayscale variation was analyzed, and the detectable limit for the proposed model was precisely determined.

2.6. Grayscale measurement

The optical detection system for the grayscale measurement is shown in Fig. 2. A commercial flatbed scanner (Scanjet 3400C) was purchased from Hewlett-Packard, USA. The grayscale depth was set to 8 bits, resulting in 256 values for each grayscale variation. The grayscale values of 0 and 255 correspond to black to white, respectively. The image caption was patterned as a circular area with 4060 pixels to fit the reaction well on the slide. After silver precipitation, the grayscale values were immediately measured with the flatbed scanner and analyzed with Adobe Photoshop® software.

3. Results and discussion

3.1. Determination of IgG–AgNP conjugate formation

Two approaches were used to confirm that the IgG was conjugated to the AgNPs. First, absorption spectrum values of the AgNPs and IgG–AgNP conjugates were measured with an UV/vis absorption spectrometer (Agilent Technology, USA). The dashed line represents the spectrum value of the 10 nm AgNP solution, and the solid line represents the spectrum value of the IgG–AgNPs conjugate solution, as shown in Fig. 3(a). The formation of IgG–AgNP conjugates was demonstrated by a red shift in the absorption peak from 390 nm (10 nm AgNPs) to 400 nm, indicating a successful conjugation between the 10 nm silver nanoparticles and the IgG molecules [39]. Second, the conjugation between the 20 nm AuNPs conjugated with Protein A and the 10 nm AgNPs conjugated with IgG was observed by transmission electron microscopy (TEM). Because both the Protein A and IgG had the specificity and conjugation, the gap size between the 20 nm AuNPs and 10 nm AgNPs could be observed, as shown in Fig. 3(b). The specific gap size formed by conjugation of the IgG with AgNPs (Fig. 3(d)) and Protein A with AuNPs (Fig. 3(e)) was demonstrated by TEM, as shown in Fig. 3(f). Therefore, the formation of IgG–AgNP conjugates was confirmed by both UV/vis spectrometry and TEM.

3.2. Reduction of silver ions catalyzed by AgNPs and IgG–AgNP conjugates

To test the applicability of the developed immunoassay, the catalytic ability of the AgNPs and IgG–AgNP conjugates to reduce silver ions to metallic silver was determined. For the AgNPs (30, 90, 150, and 300 μM), a real-time color change of the silver enhancement solution was observed, as shown in Fig. 4(a). The silver precipitation reaction could be observed from 1 min to 10 min by the naked eye, even at an AgNP concentration of 30 μM. At the highest concentration of the AgNP solution, the grayscale values reached the saturation point after 1 min, indicating that all of the silver ions appeared to be reduced to metallic silver by AgNP catalysis (Fig. 4(b)). When the concentration was lowered to 30 μM, the change in the grayscale values was similar to the previous results, but the saturation point was reached after 7 min. In these experiments, the AgNPs were found to be ideal catalysts for the reduction of the silver ions in the silver enhancement solution to amplify the optical detection signals. Even when the concentration of the AgNPs was lowered to the micromolar range, the silver ions could still be reduced to metallic silver.

For the IgG–AgNP conjugates (30, 90, 150, and 300 μM), a real-time color change was also observed from 1 min to 16 min by the naked eye, even at 30 μM of the IgG–AgNP conjugates, as shown in Fig. 5(a). When the concentration of the IgG–AgNP conjugates

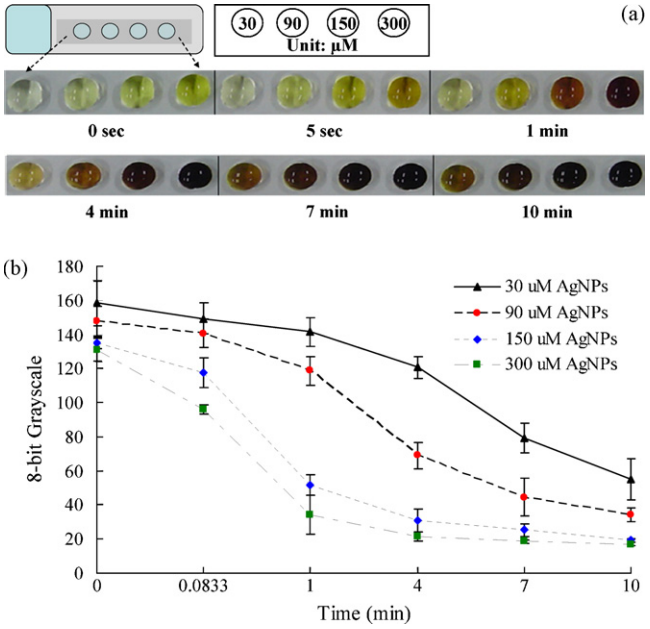

Fig. 4. (a) Real-time color change of the silver enhancement solution, which was catalyzed by AgNPs. The AgNP concentrations were 30, 90, 150, and 300 μM (from left to right). (b) The 8-bit grayscale values of the different concentrations were changed due to silver precipitation.

was 300 μM, the grayscale values reached the saturation point after 13 min, indicating that all of the silver ions were reduced to silver metal by IgG–AgNP conjugate catalysis (Fig. 5(b)). When the concentration was lowered to 30 μM, the grayscale value changes were less obvious than that of other IgG–AgNP conjugate concentrations. Therefore, the IgG–AgNP conjugates were also found to be ideal catalysts for the reduction of silver ions in the silver enhancement solution to metallic silver. Apparently, the IgG–AgNP conjugates retained the catalytic ability of the AgNPs even after conjugation.

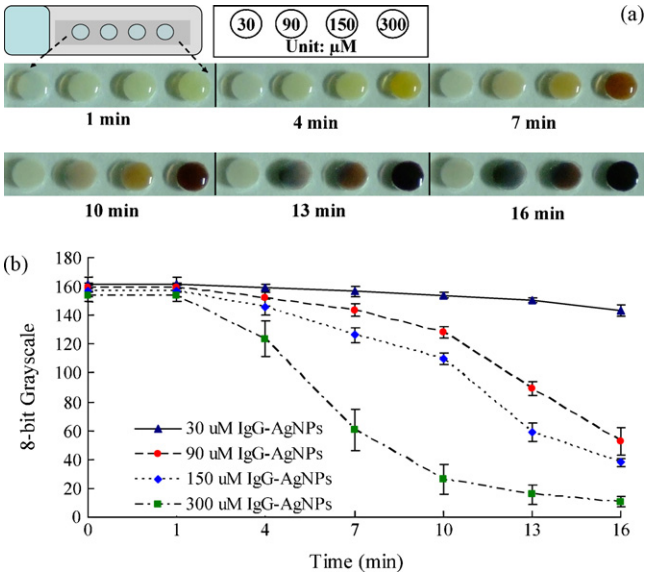

Fig. 5. (a) Real-time color change of the silver enhancement solution, which was catalyzed by IgG–AgNP conjugates. The IgG–AgNPs conjugate concentrations were 30, 90, 150, and 300 μM (from left to right). (b) The 8-bit grayscale values of the different concentrations were changed due to silver precipitation.

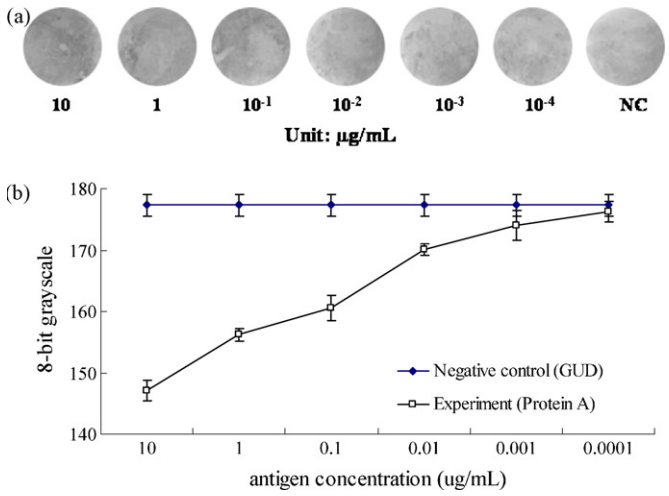

Fig. 6. (a) The difference between the Protein A concentrations (10 to 10^{-4} μg/mL) and the negative control can be easily observed by the naked eye. (b) Grayscale value changes of the sandwich immunoassay with different concentrations of antigen. These results show that the detectable concentration limit was 1 ng/mL.

3.3. Sandwich immunoassay

Our newly developed sandwich immunoassay is similar to the common sandwich format of the ELISA. The differences between these two procedures involve the antigen labeling technique (enzymes vs. AgNPs) and the signal amplification detection method. Our immunoassay provides both qualitative and quantitative analyses. In this assay, 10 μg/mL of IgG (1st antibody) was immobilized on a slide as the first layer for binding Protein A (antigen). Then, various concentrations of Protein A were immobilized on the IgG layer as the second layer. The Protein A concentrations used were 10, 1, 10^{-1}, 10^{-2}, 10^{-3}, and 10^{-4} μg/mL. Finally, 300 μM of the IgG–AgNPs conjugate solution was added in the reaction wells as the third layer. This layer was responsible for generating the optical detection signals by catalyzing the reduction of the silver ions in the silver enhancement solution. Non-specific β-glucuronidase (GUD, 1 mg/mL in PBS) was used as a negative control (NC) in place of Protein A. Each experiment was performed in triplicate.

The grayscale color change could be directly observed by the naked eye, as shown in Fig. 6(a). The Protein A concentrations (from 10 to 10^{-4} μg/mL) were respectively mapped to each grayscale value, and the relationship between antigen concentration and grayscale value (optical detection signals) is shown in Fig. 6(b). Because the grayscale value of 10^{-4} μg/mL was similar to the grayscale value of the negative control experiment (negative control: 179.33, 10^{-4} μg/mL: 178.12), the detectable concentration limit of the Protein A was determined to be 10^{-3} μg/mL.

4. Conclusion

We successfully developed a sandwich immunoassay based on the use of a flatbed scanner to detect immuno-reactive signals. AgNPs were used as antibody labels and as catalysts for silver precipitation. The silver enhancement reaction was used to magnify the optical detection signals. The detectable concentration limit for our sandwich model was determined to be 1 ng/mL, and the sensitivity is approximate to a conventional immunoassay [33–35]. Our results demonstrate that this new method is an improvement over the conventional immunoassay system in terms of easy operation, low-cost detection, requirement of only a small amount of sample, and short detection time. This newly developed experimental platform did not analyze the specific bonding between the antigen and antibody, and the bonding of both the Fab and Fc regions of IgG with the antigen should be tested and analyzed. Therefore, our newly developed immunoassay has potential applications in the clinical diagnoses of various infectious diseases.

Acknowledgments

The authors would like to thank the Center for Micro/Nano Technology, National Cheng Kung University, Tainan, Taiwan, ROC, for access to their equipment and for their technical support. Funding from the Ministry of Education and the National Science Council of Taiwan, ROC (NSC 98-2622-E-006-048-CC2, NSC 98-2622-E-006-010-C2) is gratefully acknowledged.

References

[1] J.P. Gosling, Clin. Chem. 36 (1990) 1408–1427.
[2] J.S. Rossier, H.H. Girault, Lab Chip 1 (2001) 153–157.
[3] W.C.W. Chan, S.M. Nie, Science 281 (1998) 2016–2018.
[4] M. Bruchez, M. Moronne, P. Gin, S. Weiss, A.P. Alivisatos, Science 281 (1998) 2013–2016.
[5] J. Yakovleva, R. Davidsson, A. Lobanova, M. Bengtsson, S. Eremin, T. Laurell, J. Emnéus, Anal. Chem. 74 (2002) 2994–3004.
[6] C.H. Yoon, J.H. Cho, H.I. Oh, M.J. Kim, C.W. Lee, J.W. Choi, S.H. Paek, Biosens. Bioelectron. 19 (2003) 289–296.
[7] I. Bronstein, J.C. Voyta, G.H.G. Thorpe, L.J. Kricka, G. Armstrong, Clin. Chem. 35 (1989) 1441–1446.
[8] E. Ishikawa, S. Hashida, T. Kohno, K. Hirota, Anal. Sci. 7 (1991) 891–896.
[9] B.K. Oh, J.M. Nam, S.W. Lee, C.A. Mirkin, Small 2 (2006) 103–108.
[10] Z. Peng, Z. Chen, J. Jiang, X. Zhang, G. Shen, R. Yu, Anal. Chim. Acta 583 (2007) 40–44.
[11] P.M. Lackie, Histochem. Cell Biol. 106 (1996) 9–17.
[12] O.D. Velev, E.W. Kaler, Langmuir 15 (1999) 3693–3696.
[13] R. Porter, P. van der Logt, S. Howell, M.K. Reay, A. Badley, Biosens. Bioelectron. 16 (2001) 855–875.
[14] Z. Ma, S.F. Sui, Angew. Chem. -Int. Ed. 41 (2002) 2280–2283.
[15] J.M. Nam, S.J. Park, C.A. Mirkin, J. Am. Chem. Soc. 124 (2002) 3820–3821.
[16] T.A. Taton, C.A. Mirkin, R.L. Letsinger, Science 289 (2000) 1757–1760.
[17] N.T.K. Thanh, Z. Rosenzweig, Anal. Chem. 74 (2002) 1624–1628.
[18] S. Cobbe, S. Connolly, D. Ryan, L. Nagle, R. Eritja, D. Fitzmaurice, J. Phys. Chem. B 107 (2003) 470–477.
[19] S. Schluecker, B. Kuestner, A. Punge, R. Bonfig, A. Marx, P. Stroebel, J. Raman Spectrosc. 37 (2006) 719–721.
[20] D.A. Stuart, A.J. Haes, C.R. Yonzon, E.M. Hicks, R.P. Van Duyne, IEE Proc.-Nanobiotechnol. 152 (2005) 13–32.
[21] G.C. Manara, C. Ferrari, C. Torresani, P. Sansoni, G.D. Panfilis, J. Immunol. Methods 128 (1990) 59–63.
[22] I. Alexandre, S. Hamels, S. Dufour, J. Collet, N. Zammatteo, F.D. Longueville, J.L. Gala, J. Remacle, Anal. Biochem. 295 (2001) 1–8.
[23] C.H. Yeh, C.Y. Hung, T.C. Chang, H.P. Lin, Y.C. Lin, Microfluid. Nanofluid. 6 (2009) 85–91.
[24] C.H. Yeh, H.H. Huang, T.C. Chang, H.P. Lin, Y.C. Lin, Biosens. Bioelectron. 24 (2009) 1661–1666.
[25] P.V. Kamat, J. Phys. Chem. B 106 (2002) 7729–7744.
[26] N.R. Jana, T.K. Sau, T. Pal, J. Phys. Chem. B 103 (1999) 115–121.
[27] Z.J. Jiang, C.Y. Liu, L.W. Sun, J. Phys. Chem. B 109 (2005) 1730–1735.
[28] Y.W. Cao, R. Jin, C.A. Mirkin, J. Am. Chem. Soc. 123 (2001) 1762–7961.
[29] S.J. Park, T.A. Taton, C.A. Mirkin, Science 295 (2002) 1503–1506.
[30] M. Horisberger, M.F. Clere, Histochem. Cell Biol. 82 (1985) 219–233.
[31] E. Briand, M. Salmain, C. Compere, C.M. Pradier, Colloid Surf. B: Biointerfaces 53 (2006) 215–224.
[32] L.M. Weiner, P. Carter, Nat. Biotechnol. 23 (2005) 556–557.
[33] X. Dou, T. Takama, Y. Yamaguchi, H. Yamamoto, Anal. Chem. 69 (1997) 1492–1495.
[34] Y. Ohkaru, K. Asayama, H. Ishii, S. Nishimura, N. Sunahara, T. Tanaka, K. Kawamura, J. Immunol. Methods 178 (1995) 99–111.
[35] O.G. Brakstad, J.A. Maeland, J. Med. Microbiol. 39 (1993) 128–134.
[36] Z.S. Pillai, P.V. Kamat, J. Phys. Chem. B 108 (2004) 945–951.
[37] M.V. Canamares, J.V. Garcia-Ramos, J.D. Gómez-Varga, C. Domingo, S. Sanchez-Cortes, Langmuir 21 (2005) 8546–8553.
[38] K.C. Ho, P.J. Tsai, Y.S. Lin, Y.C. Chen, Anal. Chem. 76 (2004) 7162–7168.
[39] J. Wang, R. Polsky, D. Xu, Langmuir 17 (2001) 5739–5741.